Journal of Network Intelligence ©2025 ISSN 2414-8105
Taiwan Ubiquitous Information Volume **10**, Number **2**, May **2025**

Cascading Fault Prevention Control Strategy Considering Safety and Economy Based on UPFC

Hui-Qiong Deng*
Smart Grid Simulation Analysis and Integrated Control Fujian Province Engineering Research Center,
Fujian University of Technology, Fuzhou 350118, China
dengcuifj_519@126.com

Jing-Hao Cui
Smart Grid Simulation Analysis and Integrated Control Fujian Province Engineering Research Center,
Fujian University of Technology, Fuzhou 350118, China
cuijinghao1231@163.com

*Corresponding author: Hui-Qiong Deng

Received January 13, 2024; revised June 1, 2024; accepted December 8, 2024.

Abstract. *Aiming at the problem of cascading fault caused by branch circuit interruption in the power system, and considering the limitation of only adjusting the generator output to prevent cascading fault, a cascading fault prevention control strategy based on unified power flow controller (UPFC) is proposed, which considers safety and economy. First, a cascading fault prevention control model for power systems with UPFC is proposed by selecting the safety margin index of the system by combining the operating cost of power system generation, the investment cost of UPFC and the power flow model of UPFC. A method of UPFC siting considering cascading fault prevention is proposed. The voltage phase angle and amplitude increment expressed by the UPFC control target are derived by formula, and then the sensitivity of the safety margin index to the UPFC control variable is obtained. Based on this, the installation location of UPFC is selected. Finally, the IEEE-39 bus system data is selected in MATLAB software for simulation and analysis. The simulation results show the economy and effectiveness of the predictive control strategy.*
Keywords: unified power flow controller; cascading fault; preventive control; safety margin index; economy

1. **Introduction.** The power system is expanding in scale and complexity, with the growth of residential customers leading to a continuous increase in the level of load. This has resulted in an increasingly serious concern for the security and stability of the system [1]. Cascading faults often occur after the initial fault has been resolved. The redistribution of current can cause other lines to become disconnected due to chain overload [2]. For example, the distance III section protection on the line may be triggered due to line overload action. To prevent protection malfunction caused by overload, it is effective to identify any faults on the line and block the protection that may cause interlock tripping [3,4]. However, blocking the protection on the line does not eliminate the interlocking overload state, and corresponding emergency measures are required. However, emergency control may result in economic losses if not implemented in a timely manner. Failure to control the development of the situation can also lead to major blackouts. Therefore, it is important to take preventive control measures to avoid the occurrence of secondary

faults after the initial fault. This can not only reduce or avoid the economic losses caused by emergency control but also eliminate the possible interlocking overload state after the initial fault, thus preventing the occurrence of interlocking faults [5,6].

In recent years, research on cascading fault prevention has primarily focused on adjusting generator output to achieve reasonable power flow allocation, taking into account voltage stability, system economy, and line vulnerability [7–13]. However, the preventive control method involving generator output adjustment must also consider generator start-up time, scheduling cost, and low automation levels. The Unified Power Flow Controller (UPFC) is considered the most advanced AC power flow control device. It is capable of performing independent active power flow transfer and reactive power compensation. This effectively solves the problem of uneven power flow distribution in the system. Compared to regulating generators, newly established power plants, and transmission lines, UPFC offers better economy, a high degree of automation, and stronger long-term adaptability [14]. Studies have been conducted to achieve the objectives of resilient scheduling [15], robust co-optimisation [16], and security correction [17] of power systems by using the UPFC's current regulation capability through different methods, indicating that the UPFC has favourable conditions for solving the problem of preventive control of interlocking faults. Furthermore, the power flow regulation ability of the UPFC device in the system is affected by its installation position [18]. Therefore, to fully utilise the power flow regulation ability of the UPFC, it is necessary to carefully select its installation position as a prevention control target for interlocking faults.

This paper proposes a cascading fault preventive control strategy based on UPFC, which considers safety and economy. The strategy aims to address the problems in the research of cascading fault preventive control and the related research conclusions of UPFC. The system safety is described using the safety margin index, which is selected based on the type of line protection device. A location method for UPFC is proposed with the aim of selecting an installation position that can effectively adjust the system safety margin. The article presents a cascading fault prevention and control model for power systems that includes UPFC. The model is based on the power flow calculation model of UPFC and aims to maximize the safety margin index while minimizing the system operation cost. An example using the IEEE-39 node system data is provided to verify the effectiveness of the proposed preventive control strategy.

2. Control Model for Cascading Fault Prevention in Power Systems with UPFC.

2.1. Power system safety margin index.

After the initial fault occurs, the occurrence of a secondary fault depends on the action value of the system protection device. It is not possible to quantify the safety margin of the system operation solely based on whether the state quantity exceeds the limit. This paper uses the distance protection section III with offset circular characteristics as an example. It defines the safety margin index of the remaining branches after the opening of a branch of the system to judge whether the interlocking trip occurs in any other branch L_{ij} [19].

$$Z_{ij.dist} = Z_{ij} - \frac{1}{2}(1-\alpha)Z_{set} - \left|\frac{1}{2}(1+\alpha)Z_{set}\right| \tag{1}$$

Where, the impedance of branch ij is represented by Z_{ij}, while α represents the offset coefficient and Z_{set} represents the setting value of distance protection section III.

The system's safety margin index is obtained by considering all branches based on Equation (1):

$$Z_{sys} = \min(Z_{ij.dist}) \tag{2}$$

The system safety margin index can directly show the safety of the system after the fault and whether the cascading fault occurs.

2.2. **Power System Power Flow Calculation Model with UPFC.** The Unified Power Flow Controller (UPFC) is made up of a Static Synchronous Compensator (STATCOM) connected in parallel and a Static Synchronous Series Compensator (SSSC) connected in series, back-to-back, by a DC capacitor. The series side is equivalent to a voltage source connected in series on the branch, while the parallel side is equivalent to a current source connected in parallel on the bus to the left of the branch. UPFC does not generate or consume active power, but only transfers it between the series and parallel sides. It can, however, perform independent reactive power compensation. Figure 1 shows the equivalent circuit [20].

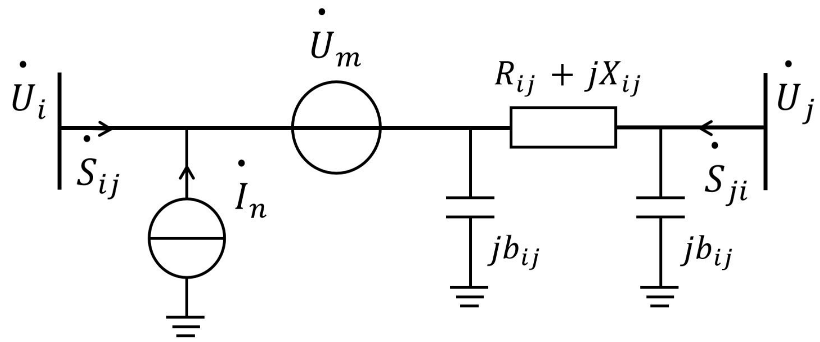

Figure 1. Equivalent Circuit of UPFC

Figure 1 shows the node voltages $\dot{U}_i$ and $\dot{U}_j$ on both sides of the branch, the equivalent voltage source $\dot{U}_m$ on the series side of UPFC, the equivalent injection current source $\dot{I}_n$ on the parallel side, and the transmission power $\dot{S}_{ij}$ and $\dot{S}_{ji}$ on the left and right sides of the branch respectively after UPFC installation. The branch resistance, reactance, and susceptance are denoted by R_{ij}, X_{ij}, and b_{ij} respectively.

The UPFC has the ability to control power flow. It controls the power extracted from the receiving end of the installation line to a fixed value of $P_c + jQ_c$. Additionally, the transmitting end can be controlled to a fixed equivalent injected reactive power Q_n or a constant node voltage amplitude U_{set} due to the reactive power compensation effect of UPFC.

$$\begin{gathered} P_{ji} = P_c \\ Q_{ji} = Q_c \\ U_i = U_{set} \quad or \quad Q_{ij} = Q_n \end{gathered} \tag{3}$$

The control objective is achieved in engineering by controlling the voltage vectors on the series and shunt side of the UPFC, which can be calculated from the equivalent circuit of Figure 1 by the knowledge of circuit theory.

When the voltage amplitude of the left node is controlled by the Unified Power Flow Controller (UPFC) to maintain a constant, the node is converted into a photovoltaic (PV) node. As a result, the reactive power transmitted by it does not participate in the iterative process of power flow calculation. The active power P_{ij} transmitted can be represented by P_c and Q_c [21].

$$P_{ij} = R_{ij}\left(\frac{P_c^2 + Q_c^2}{U_j^2} + b_{ij}^2 U_j^2 + 2b_{ij}Q_c\right) - P_c \tag{4}$$

The installation branch of the Unified Power Flow Controller (UPFC) is removed from the system and replaced with nodal injection powers P_c, Q_c and P_{ij}. As a result, the system's node power balance equation only requires additional injection power at the UPFC installation position. Since node i is a PV node and P_c and Q_c are constants, the Jacobian matrix increment caused by the additional active power injection of node i only needs to be increased during power flow calculation.

$$\frac{\partial P_{ij}}{\partial U_j} = R_{ij}\left(-2\frac{P_c^2 + Q_c^2}{U_j^3} + 2b_{ij}^2 U_j\right) \tag{5}$$

2.3. **Cascading Fault Prevention Control Model Based on UPFC.** Equations (6-7) provides the operating costs for generator generation and the investment costs for UPFC [22, 23, 24]:

$$cost_G = \sum_{g=1}^{gn}\left(a_g P_g^2 + b_g P_g + c_g\right) \tag{6}$$

$$\begin{cases} cost_{UPFC}^1 = 0.0003S^2 - 0.2691S + 188.22 \\ cost_{UPFC} = 1000S * cost_{UPFC}^1 / 8760 * y \end{cases} \tag{7}$$

Where $cost_G$ represents the cost of generating electricity, P_g represents the active output of the gth generator, and a_g, b_g, and c_g represent the coefficients of the generator's operation cost. $cost_{UPFC}^1$ represents the investment cost per unit capacity of UPFC, rewritten in the same units as the cost of generator output, multiplied by the capacity and divided by the number of years of planned use, y, and the number of hours per year, and converted into the same form as the cost of generator operation written as $cost_{UPFC}$. The unit is $\$/h$, and S represents the UPFC capacity.

Using Equations (6-7), the operating cost of the system can be written as:

$$cost = cost_G + cost_{UPFC} \tag{8}$$

To prevent cascading fault, the objective is to ensure that the safety margin index remains above zero even after the initial system fault. The objective function for controlling cascading fault prevention can be derived from Equations (2) and (8).

$$\begin{cases} f_1 = max(Z_{sys}) \\ f_2 = min(cost) \end{cases} \tag{9}$$

When multiple initial faults are selected, the minimum value of the system safety margin after each initial fault occurs shall be considered:

$$f = max\left(min(Z_{sys,1}, \ldots, Z_{sys,n})\right) \tag{10}$$

At the same time, it is necessary to satisfy the power flow constraints of the system. The power flow constraints at nodes without UPFC installed are:

$$\begin{cases} P_i = V_i \sum_{j=1}^{n-1} V_j \left(G_{ij}\cos\theta_{ij} + B_{ij}\sin\theta_{ij}\right) \\ Q_i = V_i \sum_{j=1}^{n-1} V_j \left(G_{ij}\sin\theta_{ij} - B_{ij}\cos\theta_{ij}\right) \end{cases} \tag{11}$$

When considering nodes equipped with UPFC, it is important to take into account the equivalent injection power of UPFC:

$$\begin{cases} P_i - \Delta P_c = V_i \sum_{j=1}^{n-1} V_j \left(G_{ij}\cos\theta_{ij} + B_{ij}\sin\theta_{ij}\right) \\ Q_i - \Delta Q_c = V_i \sum_{j=1}^{n-1} V_j \left(G_{ij}\sin\theta_{ij} - B_{ij}\cos\theta_{ij}\right) \\ Q_i - \Delta Q_n = V_i \sum_{j=1}^{n-1} V_j \left(G_{ij}\sin\theta_{ij} - B_{ij}\cos\theta_{ij}\right) \end{cases} \tag{12}$$

In addition to the aforementioned requirements, UPFC also requires inequality constraints for voltage amplitude, generator output, and equivalent injected power and capacity:

$$\begin{cases} P_{Gi.min} \le P_{Gi} \le P_{Gi.max} \\ Q_{Gi.min} \le Q_{Gi} \le Q_{Gi.max} \\ U_{i.min} \le U_i \le U_{i.max} \\ \Delta P_{c.min} \le P_c \le \Delta P_{c.max} \\ \Delta Q_{c.min} \le Q_c \le \Delta Q_{c.max} \\ \Delta Q_{n.min} \le Q_n \le \Delta Q_{n.max} \\ S \le S_0 \end{cases} \tag{13}$$

The formula defines $P_{Gi.max}$, $P_{Gi.min}$, $Q_{Gi.max}$, and $Q_{Gi.min}$ as the upper and lower limits of active and reactive power output from the generator, respectively. $U_{i.max}$ and $U_{i.min}$ represent the upper and lower limits of node voltage modulus. $\Delta P_{c.max}$, $\Delta P_{c.min}$, $\Delta Q_{c.max}$, $\Delta Q_{c.min}$, $\Delta Q_{n.max}$, $\Delta Q_{n.min}$ denote the upper and lower limits of equivalent series side extracted power and the upper and lower limits of parallel side constant injected reactive power of UPFC. S represents the apparent power of UPFC calculated by UPFC control quantities P_c and Q_c under the current operation state, while S_0 represents the capacity of UPFC.

By combining an objective function with equality and inequality constraints, the model for preventing cascading fault can be abbreviated as:

$$\begin{cases} f_1 = max(min(Z_{sys,1}, \ldots, Z_{sys,n})) \\ f_2 = min(cost) \\ s.t. \quad H_1 = 0 \\ \qquad\;\; H_2 \le 0 \end{cases} \tag{14}$$

Where H_1 and H_2 represent the constraints of the inequalities in Equations (10-13).

2.4. **Process for Solving the Preventive Control Model.** Multi-Objective Particle Swarm Optimization (MOPSO) is a widely used method for solving multi-objective optimization problems due to its fast convergence speed and convenient parameter setting [25].

This paper employs MOPSO to solve the cascade fault prevention control model. The position parameters of particles are taken as the output of each generator and the control parameters of UPFC, while the adaptability is measured by the safety margin index and operation cost of the system. During the iterative process, if there is no solution or the electrical quantity exceeds the limit for individual particles, the safety margin index is set to a negative value and the operation cost is set to a large value. The elimination process is then carried out to determine the dominant solution. In order to determine the adaptation degree of the multi-objective optimization algorithm, the safety margin index is calculated for each initial fault at every iteration, and the minimum safety margin is selected. This ensures a balanced approach to considering multiple initial faults. The optimal solution set is output when the maximum iteration number is reached. Please refer to Figure 2 for the flowchart.

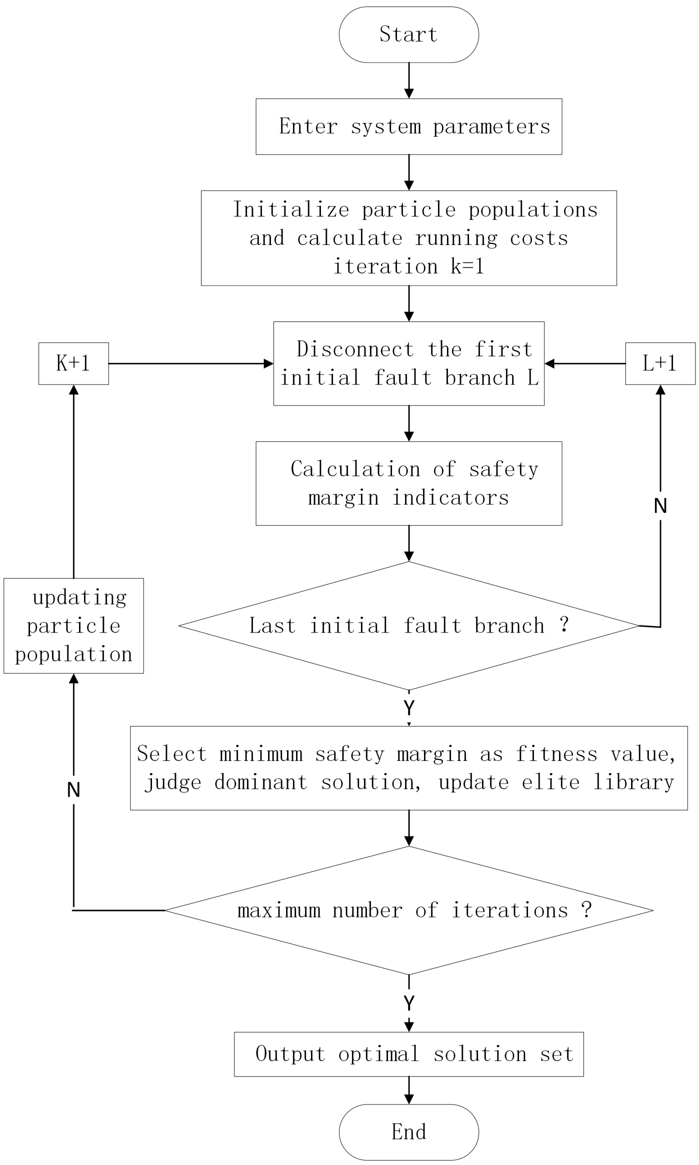

Figure 2. Flow Chart of Preventive Control Strategy

3. UPFC site selection. In order to fully utilise the power flow control capability of UPFC, it is necessary to determine the sensitivity of the system power flow distribution rationality index to the UPFC control parameters under different installation positions, and select the position with the highest sensitivity to install the UPFC.

The active power flow performance index is used to evaluate the rationality of active load distribution. It is also used to calculate the sensitivity of the index to UPFC control parameters, which serves as the basis for UPFC site selection. The expression for the active power flow performance index is:

$$PI = \sum_{L}^{nl} \frac{\omega_n}{2n} \left(\frac{P_L}{P_{L.max}} \right)^2 \tag{15}$$

The active power transmitted by branch L is represented by P_L. $P_L \cdot P_{L.max}$ represents the upper limit of branch active power. ω_n represents the branch importance coefficient, n represents the network structure coefficient, and nl represents the number of branches.

In the previous section, the voltage amplitude of the parallel side node is kept constant at U_{set} due to the reactive power compensation effect of UPFC during power flow calculation. This node is equivalent to a PV node and does not participate in reactive power iteration during power flow calculation. However, when the node voltage amplitude is used as a control variable, it cannot be considered the same as the extracted power controlled at the series side. In this section, we consider the parallel side node as the PQ node, and the UPFC controls the parallel side node by fixing the injected reactive power Q_n as the control variable at the parallel side.

In steady state, the power balance equation is satisfied, and the equivalent injection power is only increased at the location where UPFC is installed:

$$\begin{cases} \Delta P_i = P_{ij} \\ \Delta P_j = P_c \\ \Delta Q_i = Q_n \\ \Delta Q_j = Q_c \end{cases} \tag{16}$$

The Newton-Raphson formula yields:

$$\begin{bmatrix} \Delta\theta \\ \Delta U/U \end{bmatrix} = J^{-1} \begin{bmatrix} \Delta P \\ \Delta Q \end{bmatrix} \tag{17}$$

The amplitude and phase angle of the node voltage can be expressed as the sum of the constant initial value before UPFC action and the increment during UPFC action:

$$U_i = U_{i0} + \Delta U_i \tag{18}$$

Thus, it is possible to obtain the sensitivity of voltage amplitude and phase angle to UPFC control parameters.

$$\begin{cases} \frac{\partial U}{\partial P_c} = \frac{\partial \Delta U}{\partial P_c}, & \frac{\partial \theta}{\partial P_c} = \frac{\partial \Delta U}{\partial P_c} \\ \frac{\partial U}{\partial Q_c} = \frac{\partial \Delta U}{\partial Q_c}, & \frac{\partial \theta}{\partial Q_c} = \frac{\partial \Delta U}{\partial Q_c} \\ \frac{\partial U}{\partial Q_n} = \frac{\partial \Delta U}{\partial Q_n}, & \frac{\partial \theta}{\partial Q_c} = \frac{\partial \Delta U}{\partial Q_n} \end{cases} \tag{19}$$

In Equation (17), $\frac{d\Delta U}{dP_c}$, $\frac{d\Delta U}{dQ_c}$, and $\frac{d\Delta U}{dQ_n}$ represent the values corresponding to the positions of the sensitivity matrix J^{-1}.

The formula for calculating the sensitivity of P_{ij} to UPFC control parameters is based on the branch active power.

$$\begin{cases} \frac{dP_{ij}}{dP_c} = \frac{\partial P_{ij}}{\partial U} \frac{\partial U}{\partial P_c} + \frac{\partial P_{ij}}{\partial \theta} \frac{\partial \theta}{\partial P_c} \\ \frac{dP_{ij}}{dQ_c} = \frac{\partial P_{ij}}{\partial U} \frac{\partial U}{\partial Q_c} + \frac{\partial Z_{ij}}{\partial \theta} \frac{\partial \theta}{\partial Q_c} \\ \frac{dP_{ij}}{dQ_n} = \frac{\partial P_{ij}}{\partial U} \frac{\partial U}{\partial Q_n} + \frac{\partial P_{ij}}{\partial \theta} \frac{\partial \theta}{\partial Q_n} \end{cases} \tag{20}$$

The formula calculates the partial derivatives of branch active power P_{ij} to voltage amplitude and phase angle using $\frac{\partial P_{ij}}{\partial U}$ and $\frac{\partial P_{ij}}{\partial \theta}$. It is important to use clear and concise language when describing technical formulas.

Equation (15) shows how the UPFC control parameters affect the sensitivity of the active performance index.

$$\begin{cases} \frac{dPI}{dP_c} = \sum_L^{nl} \frac{\omega_n}{n} \left(\frac{P_L}{P_{L.max}} \right) \frac{dP_L}{dP_c} \\ \frac{dPI}{dQ_c} = \sum_L^{nl} \frac{\omega_n}{n} \left(\frac{P_L}{P_{L.max}} \right) \frac{dP_L}{dQ_c} \\ \frac{dPI}{dQ_n} = \sum_L^{nl} \frac{\omega_n}{n} \left(\frac{P_L}{P_{L.max}} \right) \frac{dP_L}{dQ_n} \end{cases} \quad (21)$$

Equation (20) can be used to obtain $\frac{dP_L}{dP_c}$, $\frac{dP_L}{dQ_c}$, and $\frac{dP_L}{dQ_n}$.

Finally, the sensitivity of the active power flow performance index to UPFC control parameters ($P_{ij.sens}$) can be obtained by summing the equations above.

$$P_{ji.sens} = \frac{dPI}{dP_c} + \frac{dPI}{dQ_c} + \frac{dPI}{dQ_n} \quad (22)$$

3. **Simulation example.** To verify the effectiveness of the preventive control strategy, the IEEE-39 bus system data is selected for simulation analysis in MATLAB software. The system structure and node number are shown in Figure 3, and the branch number is compiled with L.

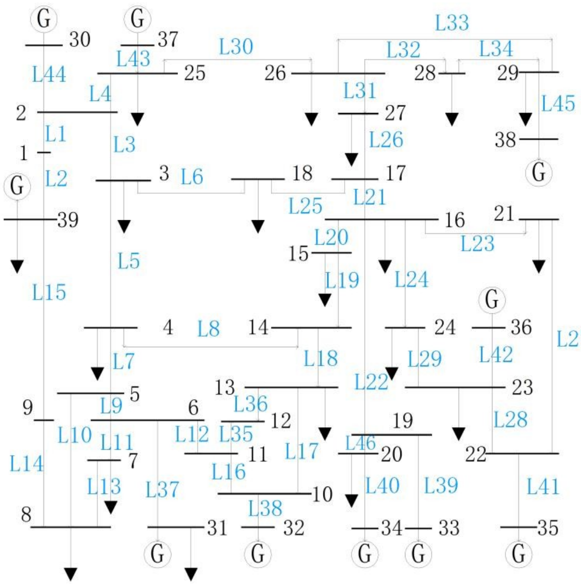

Figure 3. IEEE-39-node System Diagram

3.1. **UPFC installation location.** The branch directly connected to the generator can adjust the line power flow by adjusting the output of the generator, and the generator is used as a reactive power supply, and the connected branch does not need reactive power compensation, so UPFC does not need to be installed in the above branch, so branch L2, L15 and L37–L45 are deleted during selection.

Using Equations (27–28), calculate the sensitivity index Z_{sens} of the UPFC at different installation positions. The results are shown in Table 1, in order from largest to smallest. Due to space limitations, only the first 5 branches and index values are shown.

Table 1. Sensitivity Index of Different UPFC Installation Positions

Branch number	$P_{ij,\text{sens}}$
L21	3.212
L23	2.331
L12	1.723
L27	1.341
L14	1.029

According to the sensitivity index, branch L21 is selected as the installation branch of the UPFC. The constant volume of the UPFC is not considered in this paper.

3.2. **Economic comparison of cascading fault prevention with generator control only.** In order to verify the superiority of UPFC in preventing cascading faults compared to only regulating generators, the lowest economy and the highest safety margin are taken as the objectives for comparison. The generator generation cost is taken as the system operating cost when only regulating generators are considered, and the sum of the generator operating cost and the UPFC investment cost is taken as the system operating cost when UPFC is considered. The results are presented in Figure 5. The abscissa is the safety margin index and the ordinate is the system operating cost.

From the comparison chart, it can be seen that for the same safety margin, the operating cost of the system after considering UPFC is significantly reduced, and the optimisation range of the safety margin index is also expanded, and the optimisation effect of the safety margin index is also improved.

The maximum system safety margin obtained by controlling only the generator output and considering the UPFC without considering the generation operating cost is shown in Table 1 and the corresponding generation operating cost of the system is given. It can be seen from the results in Table 1 that the system safety margin is significantly increased and the system operating cost is significantly reduced when considering the UPFC results compared to just controlling the generator output. Therefore, it can be seen that the method in this paper has certain advantages over only controlling the generator output to prevent cascading faults.

The results obtained above can be verified when all branches are disconnected as initial faults, and space is limited to show the results when one branch is disconnected. In the process of comparative optimisation, multi-objective particle swarm optimisation (MOPSO) is chosen as the solution, and the contents of MOPSO are not discussed. See the relevant contents in the literature [25].

Table 2. Results of Safety Margin Optimization and Comparison of Economies

	Operating costs	**Safety margin**
Considering UPFC	508.65	0.1627
Adjust generator only	632.14	0.1355

4.3. Simulation results of UPFC-based cascading fault prevention control. MOPSO is used to solve the optimal UPFC control parameters and generator power. In this example, the particle population is set to 50, the iteration number is 100, and the capacity of the series side and parallel side of the UPFC is equal, which is 60MVA.

It can be seen from Figure 3 that the system will be divided into two parts after the $L22$ and $L46$ branches are disconnected, and the generator will stop operating after the

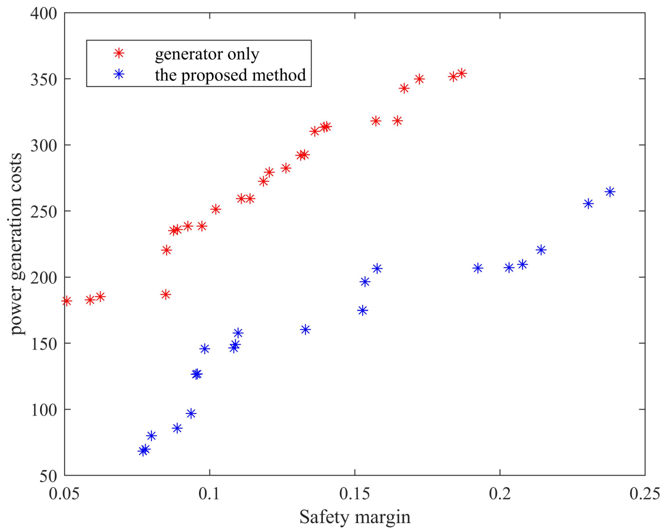

Figure 4. Comparison of Economics With and Without UPFC

$L37$-$L45$ line directly connected to the generator is disconnected, so the above branches are not considered in this paper. According to the power flow calculation, the system safety margin is less than zero after branches $L3$, $L5$, $L14$ and $L15$ are disconnected, and the system safety margin is very small after branches $L10$ and $L11$ are disconnected. If the system is disturbed, cascading faults may occur. Therefore, the above six branches are selected as initial fault branches to verify the effectiveness of the method in this paper.

In this paper, it is assumed that the measured impedance value of the branch where the UPFC is located is reasonably adjusted, the influence of the UPFC on the measured impedance is eliminated, the relay protection device can operate correctly, and the UPFC can automatically disconnect from the system when an external UPFC fault occurs [26]. Therefore, the simulation process should ensure that if the branch where the UPFC is located is disconnected due to a fault, the safety margin of the remaining branches is not less than zero under the current operating condition.

The optimised solution set is shown in Figure 5. The compromise solution is obtained by calculating the degree of membership in the literature [27]. In Figure 5, the abscissa is the system safety margin index and the ordinate is the system operating cost.

See Table 3 for the comparison results of the system safety margin index and the operating cost of each first fault branch before and after optimisation; see Table 4 for the comparison results of the UPFC control parameters and the generator power with those before control.

Table 3. Comparison of Safety Margin Indicators and Operating Costs

	Branch No.	Before	After
Safety Margin	L3	-0.0007	0.0976
	L5	-0.0026	0.0816
	L14	-0.0252	0.1070
	L15	-0.0119	0.0769
	L10	0.0038	0.1749
	L11	0.0015	0.1749
Cost		961.294	777.379

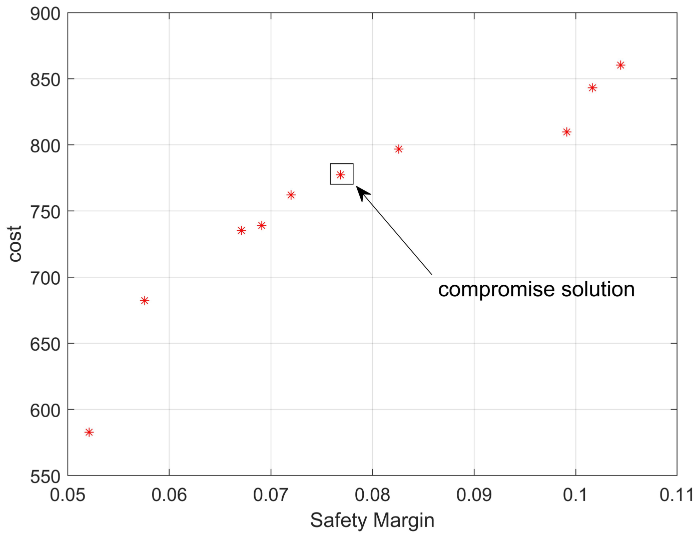

Figure 5. Optimal Solution Set and Compromise Solution

Table 4. Generator Output Comparison and UPFC Control Parameters

		Before	**After**
Generator No	G30	250	13.112
	G31	572.8	184.665
	G32	650	949.413
	G33	632	152.578
	G34	508	987.51
	G35	650	398.831
	G36	560	401.433
	G37	540	418.024
	G38	830	242.701
	G39	1000	889.202
UPFC Control Parameters	P_c		5.1488
	Q_c		-11.751
	U_{set}		0.971

Table 3 shows that the installation of UPFC, along with adjustments to its control parameters and generator output, significantly improves the system's safety margin after each initial fault branch is opened. This relieves the emergency state after branch opening and leaves a certain safety margin, while also reducing the system's operating cost. The optimization process takes into account both the system's safety and economy.

To ensure the method's universality, MOPSO is used to optimize the generator and UPFC configuration after adjusting the operating point. Figure 6 shows the optimal solution set and compromise solution. Please refer to Tables 5 and 6 for a comparison of the safety margin index, generator output, and UPFC control parameters before and after optimization.

Table 5 shows that the preventive control strategy outlined in this paper remains effective under different operating states. Therefore, the preventive control strategy for cascading fault based on UPFC, which considers safety and economy, can adapt to various operating states of the system. It ensures that the system has sufficient safety margin

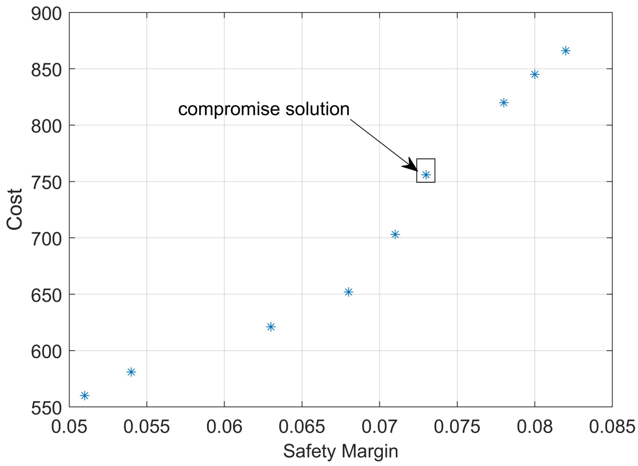

Figure 6. Optimal Solution Set and Compromise Solution after Changing Operation Point

Table 5. Comparison of Safety Margin and Operating Cost after Changing Operating point

	Branch No.	Before	After
Safety Margin	L15	-0.0013	0.0846
	L14	-0.0024	0.0783
	L25	0.0002	0.0930
	L27	0.0019	0.0842
Cost		1023.231	834.732

after adjustment, reduces operating costs, and effectively prevents the occurrence of cascading fault.

Table 6. Generator Output Comparison and UPFC Control Parameters after Changing Operating Point

Generator No.	Before	After
G30	250	112.343
G31	572.8	123.723
G32	650	725.734
G33	632	123.783
G34	508	327.476
G35	650	692.341
G36	560	301.245
G37	540	523.144
G38	830	122.632
G39	1000	891.254
UPFC Control Parameters		
P_c		11.224
Q_c		-22.245
U_{set}		1.032

4. **Conclusion.** In order to solve the problem of cascading faults caused by line break, considering the limitation of only controlling the generator output, this paper proposes a cascading fault prevention control strategy based on UPFC considering safety and economy, which reduces the operating cost of the system based on cascading fault prevention. Specific conclusions are set out below:

1) By calculating the sensitivity of the measured impedance of the branch circuit to the UPFC control parameter and selecting the installation location of the UPFC, it is possible to effectively regulate the system safety margin index through the UPFC.

2) Considering the UPFC chain fault prevention and control strategy compared to only regulating the generator output, due to the UPFC's current regulation effect can replace part of the generator output effect, the economy is better, and formulating the prevention and control strategy for the initial faulty branch circuit whose safety margin is less than zero or close to zero can effectively improve the system safety after the occurrence of the various initial faults, and prevent the occurrence of the chain faults.

The impact of new energy devices on the power system cannot be ignored in the new power system. Therefore, subsequent research can apply UPFC to the power system to prevent cascading failures of new energy devices.

Acknowledgment. This work was financially supported by the Natural Science Foundation of Fujian Province (2022J01948).

REFERENCES

[1] Y. Hu, S. Xue, H. Zhang, H. Zhang, X.-X. Feng, C.-H. Tang, Y. Ling, and P. Zheng, "Analysis and enlightenment of global blackouts in the past 30 years," *Electric Power*, vol. 54, no. 10, pp. 204–210, 2021.

[2] F.-N. Hu, L.-J. Chen, and J. Chen, "Cascading failure modeling and robustness evaluation based on AC power flow," *Power System Protection and Control*, vol. 49, no. 18, pp. 35–43, 2021.

[3] R.-B. Cao, X.-Z. Dong, and S.-E. He, "Analysis on performance of Zone-III distance protection under post-fault overload," *Proceedings of the CSEE*, vol. 35, no. 13, pp. 3314–3323, 2015.

[4] H.-Z. Liu and Z.-X. Zhou, "Post-fault overload maloperation countermeasure of transmission line distance protection," *Proceedings of the CSEE*, vol. 31, no. 25, pp. 112–117, 2011.

[5] W.-S. Wang, W.-F. Lin, G.-Q. He, W.-H. Shi, and S.-L. Feng, "Enlightenment of 2021 Texas blackout to the renewable energy development in China," *Proceedings of the CSEE*, vol. 41, no. 12, pp. 4033–4043, 2021.

[6] Y.-Q. Hou, Y. Ding, M.-L. Bao, Z.-Y. Liang, Y.-H. Song, and C. Guo, "Analysis of Texas blackout from the perspective of electricity–gas coupling and its enlightenment to the development of China's new power system," *Proceedings of the CSEE*, vol. 42, no. 21, pp. 7764–7775, 2022.

[7] H.-Q. Deng, F.-G. Zeng, X.-F. Zhang, Y.-Y. Zheng, P.-Q. Li, and J.-X. Li, "A multi-objective prevention strategy for grid cascading failure based on vulnerable line screening," *Electric Power Engineering Technology*, vol. 42, no. 2, pp. 223–231, 2023.

[8] S.-B. Jiang, J. Yang, J.-X. Wang, W. Yu, P.-Y. Xie, C. Luo, and Y.-Z. Sun, "Defense strategy against large power grid cascading failure based on coordinated preventive–emergency control," *Electric Power Automation Equipment*, vol. 39, no. 12, pp. 148–154, 2019.

[9] Y.-M. Liu, X.-P. Gu, and T. Wang, "Multi-stage blocking control of power system cascading failures considering propagation path," *Electric Power Automation Equipment*, vol. 41, no. 12, pp. 151–157, 2021.

[10] H.-Q. Deng, X.-Y. Chen, J.-Y. Wu, and R.-H. Ma, "Prevention strategy of power grid considering voltage stability and cascading outage triggering," *Smart Power*, vol. 50, no. 1, pp. 1–6+36, 2022.

[11] H.-Q. Deng and X.-Y. Chen, "Research on chain fault prevention model considering voltage stability," in *Journal of Physics: Conference Series*, vol. 2179, no. 1, 2022.

[12] Y.-T. Lin, W.-Q. Zhang, Y.-M. Lin, W. Ding, M.-X. Wu, J. Tang, J.-M. Zhang, and Q. Jiang, "Control strategy of cascading failures considering the health degree of coal-fired units and load transfer," *Power System Protection and Control*, vol. 47, no. 17, pp. 101–108, 2019.

[13] H.-Q. Deng, J. Luo, C.-C. Li, P.-Q. Li, and R.-J. Zheng, "Preventive control strategy of cascading fault considering safety and economy," *Journal of Electrical and Computer Engineering*, vol. 2021, Art. 1–12, 2021.

[14] Q. Li, N.-Y. Zhang, X.-B. Wang, F.-F. Ding, and J.-B. Fu, "Review on application of flexible power flow control technology," *Electric Power Engineering Technology*, vol. 42, no. 2, pp. 50–60, 2023.

[15] H.-S. Liu, C. Wang, P. Ju, H.-Y. Li, and B. Sun, "Bi-level coordinative resilience dispatching of power system considering unified power flow controller," *Electric Power Automation Equipment*, vol. 43, no. 4, pp. 159–167, 2023.

[16] L.-Q. Shang, Z. Hui, and J.-X. Wang, "Robust scheduling collaborative optimization strategy of power system considering optimal configuration of UPFC," *Electric Power Automation Equipment*, vol. 44, no. 2, pp. 165–172, 2024.

[17] H.-Q. Zhou, Y.-T. Gu, F. Xu, Y.-S. Yan, and X.-F. Song, "Decision-making method of corrective control for wind power system with unified power flow controller based on successive approximated linear programming," *Automation of Electric Power Systems*, vol. 46, no. 8, pp. 20–28, 2022.

[18] Z.-R. Zhu, Q. Li, Z.-N. Wei, J.-B. Zhao, G.-Q. Sun, and H.-X. Zang, "Security correction model of power system with novel unified power flow controller," *Electric Power Automation Equipment*, vol. 43, no. 2, pp. 58–66, 2019.

[19] H.-Q. Deng, "Research on the safety margin of power network considering cascading tripping," *Journal of Fujian University of Technology*, vol. 14, no. 3, pp. 255–261, 2016.

[20] X. Wu, L. Wang, X. Chen, Y. Liu, J.-G. Tao, S. Teng, and X. Chen, "Comparative research on UPFC and IPFC enhancing transmission capability of a power system," *Power System Protection and Control*, vol. 48, no. 9, pp. 128–134, 2020.

[21] J. Yang, P.-C. Song, and Z. Xu, "A load flow calculation method for power systems with novel UPFC topology," *Power System Technology*, vol. 41, no. 3, pp. 888–894, 2017.

[22] M.-H. Huang, K.-J. Tang, S.-F. Dong, B. Nan, and Y.-H. Song, "Optimal power flow considering user-side carbon emission allowances based on carbon flow theory," *Power System Technology*, vol. 47, no. 7, pp. 2703–2713, 2023.

[23] L. J. Cai, I. Erlich, and G. Stamtsis, "Optimal choice and allocation of FACTS devices in deregulated electricity market using genetic algorithms," in *IEEE PES Power Systems Conference and Exposition*, 2004, pp. 201–207.

[24] Y.-T. Niu, F.-M. Zhang, Y.-L. Wei, J.-R. Wang, and G.-X. Liu, "Optimization of UPFC site selection & capacity determination algorithm considering return of investment ratio," *Smart Power*, vol. 48, no. 5, pp. 111–118, 2020.

[25] Q.-M. Yan, X.-Z. Dong, J.-H. Mu, and Y.-X. Ma, "Optimal configuration of energy storage in an active distribution network based on improved multi-objective particle swarm optimization," *Power System Protection and Control*, vol. 50, no. 10, pp. 11–19, 2022.

[26] T. Zheng, Z. Tang, Z.-X. Zhang, H.-Y. Li, and H. Cao, "Review of the influence of unified power flow controller on relay protection and countermeasures," *Power System Protection and Control*, vol. 47, no. 15, pp. 171–178, 2019.

[27] R.-H. Liu, Y.-B. Jia, K.-N. Fu, and X.-Q. Han, "Double-layer optimization for wind and energy storage capacity configuration in transmission network considering security reserve constraints," *Power System Technology*, vol. 45, no. 7, pp. 2741–2752, 2021.